

## HIGH MAGNETIC SHEAR GAIN IN A LIQUID SODIUM STABLE COUETTE FLOW EXPERIMENT A PRELUDE TO AN $\alpha - \Omega$ DYNAMO

STIRLING A. COLGATE, HUI LI, VLADIMIR PARIEV, JOHN FINN  
T-2, Los Alamos National Laboratory, Los Alamos, NM 87545; colgate@lanl.gov

HOWARD BECKLEY, JIAHE SI, JOE MARTINIC, DAVID WESTPFAHL, JAMES SLUTZ, CEBASTIAN WESTROM, BRIANNA KLEIN,  
PAUL SCHENDEL, CLETUS SCHARLE, TRAVIS MCKINNEY, ROCKY GINANNI, IAN BENTLEY, TIMOTHY MICKEY  
Department of Physics, New Mexico Institute of Mining and Technology, Socorro, NM 87801

*Draft version June 20, 2022*

### ABSTRACT

The  $\Omega$ -phase of the liquid sodium  $\alpha$ - $\Omega$  dynamo experiment at NMIMT in cooperation with LANL has successfully demonstrated the production of a high toroidal field,  $B_\phi \simeq 8 \times B_r$  from the radial component of an applied poloidal magnetic field,  $B_r$ . This enhanced toroidal field is produced by rotational shear in stable Couette flow within liquid sodium at  $Rm \simeq 120$ . The small turbulence in stable Taylor-Couette flow is caused by Ekman flow where  $(\delta v/v)^2 \sim 10^{-3}$ . This high  $\Omega$ -gain in low turbulence flow contrasts with a smaller  $\Omega$ -gain in higher turbulence, Helmholtz-unstable shear flows. This result supports the ansatz that large scale astrophysical magnetic fields are created within semi-coherent large scale motions in which turbulence plays only a smaller diffusive role that enables magnetic flux linkage.

*Subject headings:* Dynamos — MHD — turbulence

A major effort is spent world-wide on astrophysical phenomena that depend upon magnetic fields (e.g., planetary, solar, and stellar magnetic fields, x-rays, cosmic rays, TEV gamma rays, AGN jets, AGN radio lobes, and in the interpretation of synchrotron polarization and Faraday rotation maps). Yet, so far, an agreed origin of the inferred large scale magnetic flux is without resolution. One possibility is that naturally occurring large scale near-stable rotational shear flows (as in AGN accretion disks and in stars) in combination with orthogonal, transient, rotationally coherent plumes will make natural, large scale, exponentiating dynamos that produce the large scale magnetic fluxes of astrophysics. Such plumes may be driven either by star-disk collisions in AGN (Pariev 2007a) or large scale convective elements in stars (Chandrasekhar 1960).

The New Mexico  $\alpha - \Omega$  dynamo (NMD) experiment, a collaboration between the New Mexico Institute of Mining and Technology and Los Alamos National Laboratory (Colgate, et al. 2001), is designed to explore this possibility in a rapidly rotating laboratory system. The first phase ( $\Omega$ -phase) of this two phase experiment is presented here.

The complete experiment is designed to create an  $\alpha - \Omega$  dynamo (Parker 1955; Moffatt 1978; Krause & Rädler 1980) in a conducting fluid in the laboratory using coherent fluid motions closely analogous to natural fluid motions that occur in astrophysical bodies, e.g., stars, planets (Mestel 1999), and AGN (Brandenburg 1998; Pariev 2007a,b). A dynamo converts kinetic energy into magnetic energy and furthermore must be able to exponentiate a small "seed" magnetic field by many orders of magnitude. An astrophysical dynamo does so with no wires, insulation, or rigid walls, and instead is immersed in a conducting medium.

The abstraction of the two orthogonal conducting fluid

motions, shear and helicity, necessary to achieve such dynamo action is called the  $\alpha - \Omega$  dynamo. When the two motions are comparable, it is often described as a stretch, twist, and fold or "fast" dynamo, and supposedly can be produced by turbulence alone (Nordlund et al. 1992), (Zeldovich, Ruzmaikin, & Sokoloff 1983). The problem is that a turbulent dynamo must create these two orthogonal motions out of the random behavior of ideal turbulence. Fluid turbulence maximizes the generation of entropy and the diffusive flux of momentum (Tobias and Cattaneo 2008), so that a field twisted one way by turbulent eddies at one moment of time is just as likely to be twisted the opposite way the next instant, or, like momentum, will be transported diffusively.

In contrast, the coherent, differential rotation of a Keplerian accretion disk or the rotational shear at the base of the convective zone in stars can stretch and wind-up an imbedded, orthogonal magnetic flux (the  $\Omega$  effect) through a large number of turns. In both shear flows the turbulence is expected to be relatively small because of the stability imposed by either an angular momentum gradient or an entropy gradient. (An eddy must do positive work to turn over.) The advantage of a large coherent  $\Omega$ -gain is that when it is large, the corresponding  $\alpha$ -gain (the coherent helicity deformation necessary to convert a fraction of the toroidal flux back into poloidal flux) can be correspondingly smaller (inversely as  $1/(\Omega$ -gain) and still achieve exponential dynamo action.

Parker, the originator of the  $\alpha - \Omega$  dynamo concept for astrophysical dynamos, invoked cyclonic motions to produce the helicity. Moffatt (Moffatt 1978) countered that a typical atmospheric cyclone makes very many turns before dissipating, and therefore makes the sign of the  $\alpha$ -converted flux incoherent. Moffatt sought motions where the rotation angle was finite,  $\sim \pi/4$ . Greg Willette (Willette, G. T. 1994) and the first author suggested that

buoyant plumes were a unique solution to the problem of coherent dynamo helicity. Beckley et al. (Beckley et al. 2003) demonstrated this property experimentally of finite,  $\sim \pi/4$ , coherent rotation of a driven plume before it dissipated through turbulent diffusion in the background fluid. Driven plumes are planned to be used in the  $\alpha$  phase of the NMD experiment.

Two liquid sodium dynamo experiments have produced positive exponential gain, but the flows were constrained by rigid walls unlike astrophysical flows (Stieglitz 2001; Gailitis et al. 2000). The rigid walls restrict turbulent eddy size by the distance from the wall, log-law of the walls (Landau & Lifshitz 1959), thereby producing low turbulence. The three recent experiments use the Dudley-James (Dudley and James 1989) or Von Karman flow (counter rotating flow converging at the mid-plane and driven by two counter rotating propellers or vaned turbine impellers, respectively, (Forest, et al 2002; Nornburg et al. 2006; Spence et al. 2007; Lathrop et al. 2001; Petrelis et al. 2003; Odier, et al. 1998; Peffley et al. 1979)) in which free turbulence is induced by the Helmholtz instability at the shearing mid-plane. This combination of coherent motions and unconstrained shear-driven turbulence at the mid-plane,  $(\delta v/v)^2 \simeq (1/2\pi)^2$ , resulted in a maximum  $\Omega$ -gain of  $\sim \times 2$  in the mid-plane shear. Recognizing the enhanced resistivity of the mid-plane turbulence, the team at Wisconsin added a mid-plane baffle to reduce the turbulence, following which the  $\Omega$ -gain increased to  $\simeq \times 4$  (Rahbarnia et al. 2010). The von Karman Sodium 2 (VKS2) experiment in the same geometry produced exponential gain (Monchaux et al. 2007); however, this generated magnetic flux was axi-symmetric in violation of (Cowling 1981). The dynamo action was explained not by turbulence but by the production of large coherent helicity produced by the radial vortices induced by the rigid vanes of the impeller (Laguerre et al. 2008).

In contrast to these experiments the NMD apparatus was designed from the start to produce low-turbulence high shear Couette flow in the annular volume between two coaxial cylinders rotating at different angular velocities (see schematic in Figure 1), for the inner high speed cylinder and  $\Omega_2$  for the outer slow speed cylinder (with its attached end walls that confine the liquid sodium). This flow may be stable or unstable depending upon the ratio of angular velocities (stable/unstable boundary,  $\Omega \propto 1/r^2$ ). Fig. 1 also indicates the Ekman flow, a thin fluid layer flowing along the boundaries of the annular volume and including a small radial return flow from inner to outer cylinder through the fluid volume. The Ekman flow produces both a torque and a small but finite level of turbulence (Ji et al. 2001). This turbulence adds a small turbulent resistivity to that of metallic sodium. Fig. 1 also indicates the five pressure sensors distributed radially at one end. The pressure distributions, measured by the five pressure sensors, are the result of an integral of the centrifugal stress, and so are an indication of the actual rotational flow angular velocity distribution.

For the magnetic measurements, a 50 kW AC induction motor (20kW is used for stable Couette flow) drives a gear train with clutches and power take-off that rotates the two cylinders at the fixed ratio of  $\Omega_1 = 4\Omega_2$ . The outer cylinder can also be disengaged from the gear

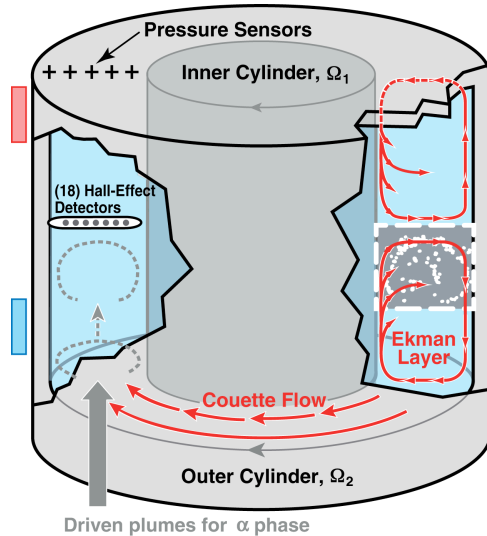


FIG. 1.— This schematic drawing of the fluid flow field of the experiment shows the inner cylinder of  $R_1 = 15.2$  cm rotating at  $\Omega_1/2\pi = 68$ Hz relative to the outer or confining cylinder of  $R_2 = 30.5$  cm at  $\Omega_2 = \Omega_1/4$ . Liquid sodium in the annular space undergoes Couette rotational flow. In addition a thin layer in contact with the cylinder walls and end walls undergoes Ekman flow, circulating orthogonally around and then through the Couette flow. Pressure sensors in the end wall and the magnetic probe housing are also shown schematically.

train by a clutch, and a DC motor used to accelerate or brake the outer cylinder independently from the driven inner cylinder. The independent drive of the outer cylinder as it speeds up or slows down allows different  $\Omega_1/\Omega_2$  ratios to be explored. The DC motor housing (stator) is mounted on bearings. A torque arm with two force sensors (+−) connects the motor stator to ground, so that the torque on the DC motor can be measured separately from the drive of the inner cylinder. This arrangement allows us to measure the torque between the two cylinders due to the Ekman flow. In particular, when the inner cylinder is driven at higher speed by the AC motor, the Ekman fluid torque tries to spin up or accelerate the outer cylinder. Two torques counteract this acceleration: 1) the friction in the bearings that support the rotation of the outer cylinder and 2) the torque on the DC motor when used as a generator, or brake. (The generated power is dissipated in a resistor.) In Fig. 2 (left) the crosses are the measurements of the braking force exerted by the DC motor torque arm; the dashed line is the calibrated bearing torque (measured by disengaging the inner cylinder drive and rotating the outer cylinder with the DC motor alone). The sum of these two torques is equal to the Ekman fluid torque spinning up the outer cylinder.

The experiment was originally designed based upon the supposition that the primary torque between the two cylinders would be due to the radial Ekman flow at the end walls and would be small,  $\sim 1/10$ , compared to pipe flow wall friction stress,  $\tau = \rho C_D v^2$ . In Fig. 2 (left) the minimal Ekman flow torque occurs at  $\Omega_1/\Omega_2 \sim < 4$ , somewhat less than the limit of stable Couette flow. The torque value is  $2 \times 10^8$  dyne-cm, close to the approximation that each Ekman layer thickness is  $\Delta \simeq R_1/Re^{1/2} \simeq 5 \times 10^{-3}$  cm and that the average radial flow velocity within the layer is  $v_r \simeq (\Omega_1 R_1)/2$ , Ji

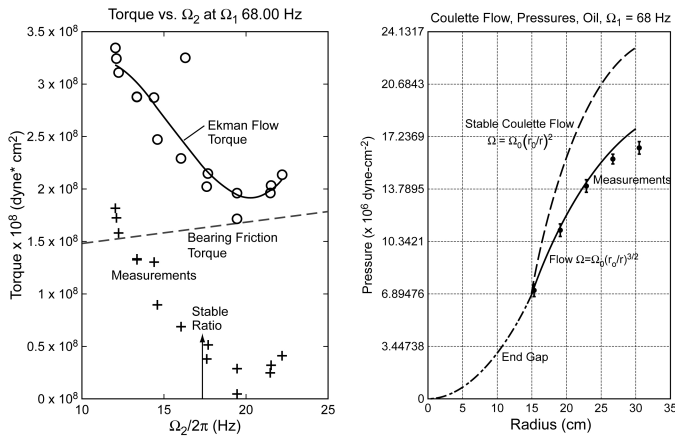


FIG. 2.— (left) The lower crosses are the measured DC generator torques; the dashed line is the measured bearings torque, and the sum of the two is the top solid curve, the torque due to the Ekman flow. With the inner cylinder driven at 68 Hz the graph of torque versus  $\Omega_2$  has a minimum close to the stable Couette ratio,  $\Omega_1 = 4\Omega_2$ , with a value of  $\sim 2 \times 10^8$  dynes-cm as predicted for two Ekman layers of thickness  $\delta_{Ek} \sim R_1/Re^{1/2} = 3 \times 10^{-4}$  cm. Fig.2 (right) compares the measured and theoretical pressures. The pressure as a function of radius in the annular Couette volume starts at  $R_1$  and extends to  $R_2$ . The finite pressure at  $R_1$ ,  $P_1 \simeq 100$ psi is due to the centrifugal pressure in the narrow gap between the inner cylinder rotating at  $\Omega_1$  and the end wall rotating at  $\Omega_2$  (dot-dash curve). From there, the pressure in the annular volume is extrapolated either as  $\Omega \propto R^{-2}$ , the upper long dash curve, or  $\Omega \propto R^{-3/2}$ , the lower solid curve. The measurements fall along the  $R^{-3/2}$  pressure distribution curve indicating less shear than ideal Couette flow.

et al. (2001).

In Fig 2 (right), the measured pressures are compared to the calculated pressures corresponding to two different angular velocity power laws. The upper (dashed) curve corresponds to ideal, maximum shear, stable Couette flow, or  $\Omega \propto r^{-2}$ , but the experimental points follow the lower solid curve corresponding to  $\Omega \propto r^{-3/2}$ . In other words, the Ekman flow torque has distorted the angular velocity profile and reduced the shear relative to ideal Couette flow. This reduced shear in the sodium partially accounts for the reduction in the  $\Omega$ -gain,  $\sim \times 8$ , versus ideal  $\Omega$ -gain  $\sim R_m/4\pi \simeq \times 20$  (Pariev 2007b). Where ideal corresponds to a single current direction versus counter current direction within the sodium in the experiment.

Turbulent flow at such high  $Re$ ,  $10^7$ , is still well beyond current simulation capability. The Ekman flow is a flux of fluid of reduced angular momentum deposited at the outer surface of the high-speed inner cylinder. The torque reducing this angular momentum is friction with the end walls, which in turn reduces the angular velocity of the Couette flow in the annular volume. Unstable flow, "pipe flow" turbulent friction with the inner cylinder surface counteracts this torque by speeding up this flow. An analysis of turbulent shear flow between two rigid walls that partially explains these results starts with the recognition that the torque in the Couette volume is a constant, independent of radius and axial position. Then this shear stress is maintained constant in two laminar sub layers (Schlichting 1960) with  $Re \simeq 100$  and maintained constant in two turbulent boundary layers in a log-law-of-the-walls solution (Landau & Lifshitz 1959). When the distance from the walls corresponds to an eddy scale of the radial gradient, a transition takes place to a

scale independent eddy size turbulent torque connecting the two regions at inner and outer boundaries. The mean velocity distribution or shear in this solution is reduced to  $\Omega/\Omega_1 \propto (R_1/R)^{1.64}$  rather than the no Ekman flow,  $\Omega/\Omega_1 = (R_1/R)^2$ .

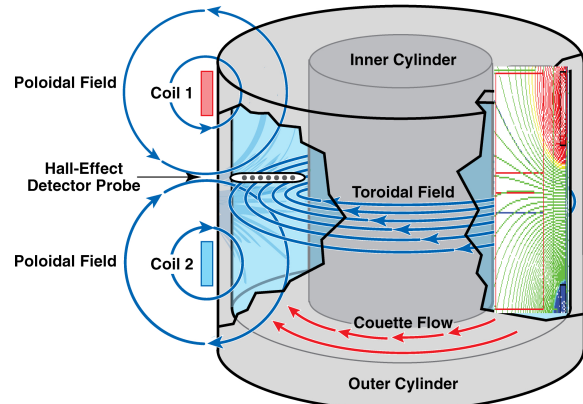


FIG. 3.— The schematic drawing shows the magnetic flux produced by two coils with current in opposition so that poloidal or radial field is produced at the mid-plane (left). Superimposed (right) are the flux lines from the Maxwell calculation with the iron shield and steel shaft included, and showing the concentration of radial flux at the mid-plane. This radial flux crosses the high shear of the Couette flow of liquid sodium producing the enhanced toroidal field. Only dimensions, iron, and coil currents are input to the Maxwell calculation. The  $B_r$  field from the Maxwell calculations agrees with the calibrated probe measurements to 10%.

The magnetic field Hall detector probe, internal to the liquid sodium at the mid-plane, is the primary diagnostic of the experiment. It consists of 6 multiple, 3-axis, magnetic field Hall effect detectors at the mid-plane in the annular space between the two cylinders and contained in an aero-dynamically shaped housing. (The fluid friction drag produced by this housing, primarily Ekman flow, is estimated to be  $\sim 0.1$  of the end-wall Ekman torque.) These magnetic detectors can measure fields from 0.1 G, the earth's field, to up 10 kG. When the initial field  $B_\phi$  is compared to the static field components of  $B_r$  instead of the expected zero when no shear exists in the conducting fluid, a cross-talk, due to misalignment of the detectors within the probe is such that  $B_\phi \simeq \pm 0.1B_r$ .

The  $\Omega$ -gain was then measured using the calibrated  $B_r$  magnetic field as a function of the coil currents. Because of the high gain, large  $B_\phi$ , and the lack of perfect orthogonality of the Hall detectors, the simultaneous measurement of the  $B_r$  field would be expected to be contaminated by a small fraction of the much larger  $B_\phi$  field. Therefore the comparison is made between the applied  $B_r$  field, calculated from the measurement of the coil currents.

Fig 4 confirms that the measurements are repeatable by showing four experiments over-laid where the  $\Omega$ -gain ratio of  $\times 8$  is repeated all with a low bias field of  $B_r \simeq 12$  G. The  $B_\phi$  produced by the Couette flow shear is of order  $B_\phi \simeq 8 \times B_r$ . We then measured whether an increase in the velocity shear in the Couette volume might increase the  $\Omega$ -gain ratio as one might naively expect. The velocity shear is increased by slowing the outer cylinder by using the DC motor as a generator or brake. The ratio  $\Omega_1/\Omega_2$  was increased by 20% or  $\Omega_2 = 14$ Hz, but the  $\Omega$ -

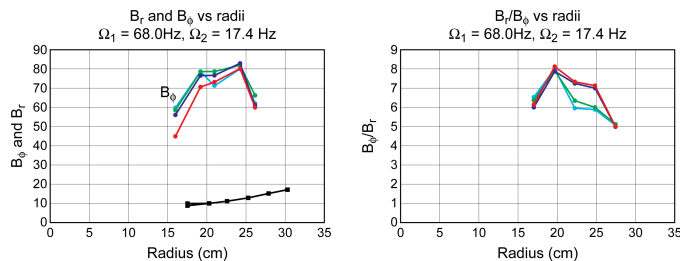


FIG. 4.— The left panel shows the magnitude in gauss of the applied radial field  $B_R$ , lower curve (in agreement with the Maxwell calculation), and the upper curves show the measured toroidal magnetic field for four over-laid experiments at  $\Omega_1 = 68$  Hz, stable Couette ratio, i.e.,  $\Omega_1/\Omega_2 = 4$  and a weak applied field,  $B_r \simeq 12$  G. The right panel shows the ratio  $B_\phi/B_r \sim \times 8$  of the same over-laid experiments.

gain remains constant. This suggests the gain expected due to shear is balanced by the greater flux diffusion due to the increased turbulence of the now unstable Couette flow (see Fig 2). Roughly 100 electronic samples are recorded and averaged during the several second recording cycle of each of four magnetic experiments. The time variation between each run reflects slight changes in the Couette flow relaxation time and hence, the angular velocity distribution. This accounts for the major fraction of the variation among the four samples shown, although one run was performed with a change in the sodium fill level. The repeatability among these four runs as well as several additional runs in the following six months gives us confidence that the conclusion of high  $\Omega$ -gain is valid.

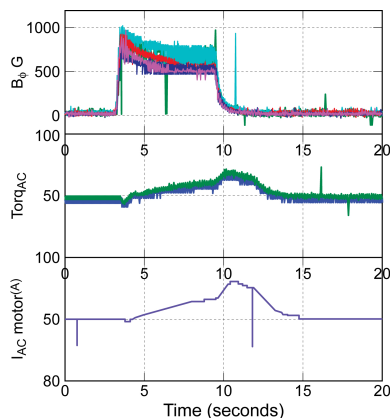


FIG. 5.— The top trace shows the derived toroidal field of  $B_\phi \sim 750$  G as a function of time from an applied radial field of  $\sim 250$  G. The  $\Omega$ -gain is now reduced to  $\times 3$ . The bottom traces are the AC motor torque and current respectively, each showing a 50% increase due to back reaction. The delay of several seconds in the back reaction torque corresponds to the spin-down time, inertia of the initial Couette flow to reach a new, perturbed velocity profile.

The expected back-reaction should occur at a value of the applied poloidal,  $B_r$ , field where the dissipation and torque of the enhanced  $B_\phi$  affects the flow field and the added torque shows up as additional current and torque in the AC drive motor. This effect is shown in Fig 5, where, in addition, the expected reduction in the  $\Omega$ -gain ratio, from  $\times 8$  to  $\sim \times 3$  is observed. A larger poloidal field is applied,  $B_r \simeq 250$  G, large enough to expect to see a back reaction due the stress of the  $B_\phi$  field. The back reaction stress will modify the Couette flow profile such as to reduce the  $\Omega$ -gain and hence reduce the back reaction stress until a new steady state is achieved at reduced  $B_\phi$ . In addition this additional stress will increase the torque, or power necessary to drive the Couette flow at constant frequency.

In Fig 5 the measured difference in power,  $\simeq 10$  kW, due to the back reaction is the power dissipated due to the resistivity of the sodium. We estimate that the magnetic field energy density,  $B_\phi^2/8\pi$ , is dissipated at  $\langle \Omega \rangle \times (Vol)$  where the volume of high  $B_\phi$  is  $\simeq (L/2)\pi \langle r \rangle^2$ . This results in a power of  $\sim 12$  kW, roughly in agreement with the measured 10 kW.

In conclusion the demonstration of large  $\Omega$ -gain in low turbulent shear in a conducting fluid transforms an applied poloidal field into a much larger,  $\times 8$ , toroidal field. This is likely to be the mechanism of the  $\Omega$ -gain of a coherent  $\alpha - \Omega$  astrophysical dynamo.

This experiment was first funded by NSF, but then a cooperative arrangement between Los Alamos Nat. Lab. and the Univ. of Calif continued this funding in cooperation with New Mexico Tech for several years of initial development. Recently funding by IGPP of LANL and NMIMT has helped. Very many undergraduate students have participated, The facilities of NMIMT, machine shop, administration, EMRTC, CMSO, and many others have made this development possible.

## REFERENCES

- Beckley, H.F., Colgate, S.A., Romero, V.D., and Ferrel, R., 2003, *Astrophys. J.*, 599, 702
- Brandenburg, A. 1998, in “Theory of Black Hole Accretion Disks”, edited by M.A. Abramowicz, G. Björnsson, & J.E. Pringle, Cambridge University Press
- Chandrasekhar, S., 1960, *Proc. Natl. Acad. Sci.*, 46, 253
- Colgate, S.A., 2006 *Astron. Nachr. / AN* 327, No. 5/6, 456–460
- Colgate, S.A., Pariev, V.I., Beckley, H.F., Ferrel, R., Romero V.D., and Weatherall, J.C. 2001, *Magnetohydrodynamics*, 38, 129.
- Cowling, T.G. 1981, *Annual Rev. Astron & Astro.*, 19, 115
- Dudley, M.L., James, R.W.: 1989, *Proc. R. Soc. London, Ser. A* 425, 407
- Forest, C.B., Bayliss, R.A., Kendrick, R.D., Nornberg, M.D., O’Connell, R., Spence, E.J.: 2002, *Magnetohydrodynamics* 38, 107
- Gailitis, A., Lielausis, O., Platcis, E., et al.: 2001, *Phys. Rev. Lett.* 84, 4365
- Ji, H., Goodman, J. & Kageyama, A., 2001, *MNRAS*, 325, L1
- Krause, F., & Rädler, K.H. 1980, *Mean-Field Magnetohydrodynamics and Dynamo Theory.* (Oxford: Pergamon Press)
- Laguerre, R., Nore, C., Riberiro, A., Guermond, J.L., Plunian, F., 2008, *PRL*, 101, 104501
- Landau, L.D. & Lifshitz, E.M., 1959, *Fluid Mechanics.* Pergamon Press, London
- Lathrop, D.L., Shew, W. L., and Sisan, D.R., 2001, *Plasma Phys. & Controlled Fusion* 43, A151
- Mestel, L. 1999, *Stellar Magnetism.* (Oxford: Clarendon)
- Moffatt, H.K. 1978, *Magnetic Field Generation in Electrically Conducting Fluids.* (Cambridge: Cambridge University Press)
- Monchaux, R ; Berhanu, M ; Bourgoïn, M ; Moulin, M ; Odier, P et al., 2007, *Phys. Rev. Lett.* 98, 044502
- Noguchi, K., Tajima, T. & Matsumoto, R., 2000, *APJ*, 541, 802
- Nordlund, A.; Brandenburg, A.; Jennings, R.L.; Rieutord, M.; and others., 1992, *APJ*, 392, 647.

- Nornburg, M.D., Spence, E.J., Kendrick, R.D., Jacobson, C.M., Forest, C.B., 2006 arXiv:physics/0510265 v2 23 Dec 2005
- Odier, P., Pinton, J.-F., and Fauve, S., 1998, Phys. Rev. E 58, 7397.
- Pariev, V.I., 2001, PhD Thesis, University of Arizona
- Pariev, IV., and Colgate, S.A., 2007, APJ, 658: 114-128.
- Pariev, IV., and Colgate, S.A., 2007, APJ, 658: 129-160
- Parker, E.N. 1955, APJ, 121, 29
- Peffley, N.L., Cawthorne, A. B. and Lathrop, D.P., 2000, Phys Rev. E, 61, 5287
- Petrelis, F., Bourgoïn, M., Burguete, J., Chiffaudel, Mari, J., Daviaud, A. F., Fauve, S., Odier, P., and Pinton, J.-F., 2003, Phys Rev. Lett, 90, 174501
- Prandtl, L. 1952, Essentials of Fluid Dynamics. Hafner Publishing Company, New York
- Rahbarnia, K., et al., 2010, Bul. APS, DPP, NP9-73, p 218
- Richard, D. & Zahn J-P, 1999, Astron. Astrophys., 347, 734
- Schlichting, H., 1960, Boundary-layer Theory. Mc Graw Hill, New York
- Spence, Nornberg, Jacobson, Parada, Kendrick, and Forest, 2007, Phys. Rev. Lett. 98 164503.
- Stieglitz, R., Müller, U.: 2001, Physics of Fluids 13, 561
- Taylor, G.I., 1936, Proc. Roy. Soc. London A, 157, 546
- Tobias, S.M., and Cattaneo, F., 2008, PRL 101, 125003
- Velikhov, E.P., 1959, Sov. Phys. JETP, 36, 995
- Wendt, F., 1933, Ing. Arch., 4, 577
- Stochastic excitation of the solar oscillations by turbulent convection. Dissertation (Ph.D.), California Institute of Technology
- Zeldovich, Ya.B., Ruzmaikin, A.A., & Sokoloff, D.D. 1983, Magnetic Fields in Astrophysics. (New York: Gordon and Breach Science Publishers)